International Journal of Pharmaceutics, 93 (1993) 101–109

IJP 03028

Factors affecting differences in film thickness of beads coated in fluidized bed units

R. Wesdyk, Y.M. Joshi, J. De Vincentis, A.W. Newman and N.B. Jain

Bristol-Myers Squibb Pharmaceutical Research Institute New Brunswick, NJ 08903 (USA)

(Received 18 February 1992)
(Modified version received 31 August 1992)
(Accepted 2 September 1992)

Key words: Fluidized bed coating; Multi-particulate system; Film thickness variation; Spray mode; Fluidization pattern; Segregation

Summary

Previous work (Wesdyk et al., *Int. J. Pharm.*, 65 (1990) 69–76) demonstrated that various size beads, dispersed in a single bed, display differences in film thickness when coated in a fluidized bed apparatus equipped with a Wurster column. The differences in film thickness were attributed to differences in fluidization patterns and velocities of the various size beads. The present study examines the effect of spray mode and process parameters on the variation of film thickness for a fixed particle size range and distribution. Beads with a size distribution in the no. 14–no. 20 mesh range were coated with an aqueous polymeric dispersion using top, bottom, and tangential spray fluidized bed units. Film thickness of the coated beads was measured using a scanning electron microscopic method. It was observed that unlike batches coated in the bottom spray (Wurster) mode, the batches coated in the top and tangential spray modes exhibited no trend in film thickness. These results are consistent with the differences observed in the surface area normalized release rates of the various size beads coated in the three spray modes. The results also indicated that for the bottom spray mode, a reduction in the atomizing air pressure, while substantially reducing differences in fluidization patterns, had only a marginal effect in reducing the differences in film thickness.

Introduction

Multi-particulate, modified release dosage forms are often desired for a variety of reasons, including improved efficacy and safety profiles. Typically, this type of dosage form consists of coated beads, or pellets, encapsulated in hard gelatin shells. The beads can be manufactured by any number of techniques including extrusion/spheronization, or powder or solution layering. However, depending on the manufacturing process the beads may not be uniform in size.

Only recently has the impact of the size distribution of the beads been examined with regards to the further processing of the pellets in a fluidized bed coater. Ragnarsson and Johnson (1988) demonstrated that if the same amount of coating is applied on two separate monodispersed (uniform size beads) particle beds of the same weight, the bed containing the smaller particles would have thinner films because the same amount of

Correspondence to: R. Wesdyk, Bristol-Myers Squibb Pharmaceutical Research Institute, One Squibb Drive, New Brunswick, NJ 08903, U.S.A.

coating must be spread over a larger surface area. This work demonstrated the importance of understanding the relationship between film thickness and batch-to-batch differences in particle size, or total surface area. The work, however, did not address the effect of particle size distribution within a single batch.

In a polydispersed system, each bead should receive an amount of film proportional to its surface area, and hence, the film thickness (amount per unit surface area) of the beads would be the same. Typically, the droplet size of the atomized coating solution is significantly smaller than the smallest bead to be coated, and therefore, the situation is analogous to leaving a large and small bucket in a rainstorm. The large bucket will receive a greater amount of water (proportional to its greater exposed surface area) than the smaller bucket, however, both buckets will contain an equal depth of water.

The relationship between film thickness and size distribution, or any other bead attribute, is extremely important. The release rate of a drug from the beads is controlled by the thickness of the film; further, free flowing beads of different sizes often segregate during handling. If the various size beads were to segregate before or during encapsulation, the potential would exist for product to vary greatly with respect to release rate, or dissolution characteristics. Therefore, it is important to understand the impact of size distribution, surface area, and mass (or density) on the film thickness of various size beads dispersed in a single bed.

Previous work conducted in our laboratories (Wesdyk et al., 1990) demonstrated that the film thickness of various size beads contained within a batch was, in fact, not uniform when coated in a fluidized bed apparatus equipped with a Wurster column (bottom spray). Larger beads received thicker films and consequently released drug at a slower rate than did the smaller beads. It was postulated that the variation of film thickness was related to differences in the fluidization patterns and velocities (non-ideal behavior) of the various size beads. It is conceivable that the design of alternate spray modes, or the modification of process parameters, might limit or decrease the potential for these differences in fluidization patterns. Thus, the present study aims to examine the impact of various fluidized bed processes, including bottom, top and tangential spray modes, on differences in film thickness of the beads of various size. The effects of selected processing parameters, including fluidizing air volume and atomizing air pressure, were also evaluated.

Experimental

Method of manufacture

A bead formulation, designed to produce a non-disintegrating core, was developed. Beads were manufactured utilizing extrusion/spheronization techniques, and screened to obtain a no. 14–no. 20 mesh cut. Sub-batches of these beads were coated in Glatt fluidized bed coater/granulators, models GPCG-5 (bottom and top spray experiments) or VersaGlatt (tangential spray experiments). Schematic diagrams of the fluid-bed coater and the various spray modes are given in Figs. 1–3. The coating was applied from commercially available aqueous polymeric systems. Typically, a 4.8% w/w film level was applied. The release controlling membrane is insoluble in the dissolution fluid (0.1 N HCl), and non-swelling in nature. Coating process parameters are given in Table 1.

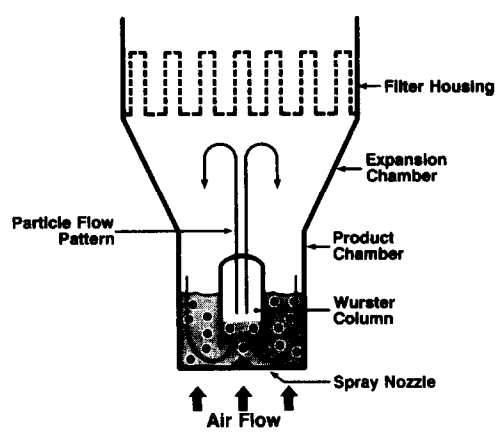

Fig. 1. Schematic diagram of a bottom spray equipped (Wurster mode) fluidized-bed coater. Not drawn to scale.

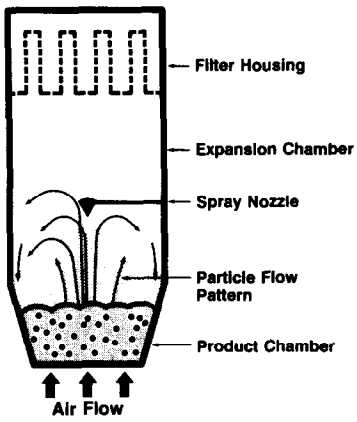

Fig. 2. Schematic diagram of a top spray equipped fluidized-bed coater. Not drawn to scale.

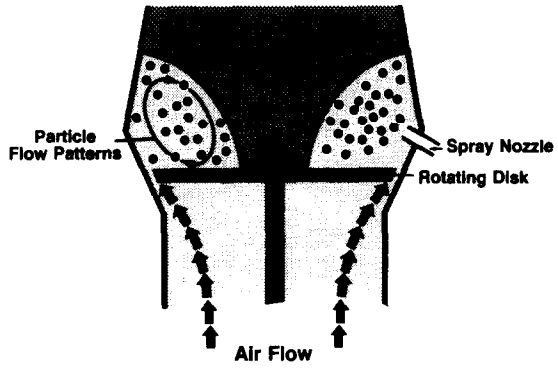

Fig. 3. Schematic diagram of a tangential spray equipped fluidized-bed coater. Not drawn to scale.

Color coding of various size beads, for purposes of monitoring segregation, was accomplished by applying a thin film into which either FD&C Red No. 3 or FD&C Blue No. 2 dye had been incorporated. The extent of segregation of the various size beads (color coded), when fluidized in the bottom spray coater, was visually monitored through viewing ports located in the product and expansion chambers. This method allowed for sufficient differentiation of the gross differences in fluidization patterns which are noted as part of this work.

Testing

Screening Beads were separated into various sized fractions by sieving through appropriate U.S. Standard mesh screens.

Particle size distribution The testing was performed on a Fritsch vibratory sieve shaker using 100 g beads at an amplitude of '4' for 3 min.

Bulk density The testing was performed on a Sargent-Welsh Volumeter. Results reported are an arithmetic mean of five measurements.

Dissolution Dissolution testing was performed using the USP basket method in 0.1 N HCl. Samples were filled into size no. 1 hard gelatin shells to yield 100 mg (drug content) po-

TABLE 1

Process parameters utilized during coating

Parameter	Bottom spray (GPCG-5)	Top spray (GPCG-5)	Tangential spray (VersaGlatt)
Charge (kg)	5	10	1
Nozzle (mm)	0.8	1.2	0.8
Partition height (inch)	3/4	N/A	N/A
Atomizing air (bar)	2.5 [a]	2.5	2.5
Product temperature (°C)	40	40	40
Spray rate (g/min)	7–11	12–18	5–8
Air volume (CFM)	60 [a]	240	N/A
Curing temperature (°C)	60	60	60
Curing time (h)	1	1	1
Plate speed (rpm)	N/A	N/A	300–700
Weight gain (%)	4.8	4.9 [b]	4.8

[a] Modified as indicated during process parameter evaluation.

[b] Modified as indicated to obtain similar (top, bottom and tangential) dissolution characteristics.

tency capsules. Amount of drug dissolved in the dissolution medium was determined by HPLC.

Scanning electron microscopy (SEM) Film thickness measurements were obtained using an Amray model 1820T SEM system. The beads were sliced into two sections, fixed onto an aluminum stage using carbon paint, and sputter coated with a Au/Pd alloy to reduce charging. The mount was placed in the vacuum chamber of the microscope, aligned, and focused for analysis. The film thickness was measured in triplicate at positions of 3:00, 6:00, and 9:00 o'clock relative to the top of the bead where the initial cut was made.

As in previous work (Wesdyk et al., 1990), EDX analysis, using an EDAX 9900 system, was utilized as a qualitative tool. This technique, as described by Brown (1986) and Ghebre-Sellassie et al. (1986), was used to monitor the extent of solubilization of core components into the film.

Coating efficiency Coating efficiency was measured as the amount of film deposited (determined by weight gain, corrected for moisture loss or gain) versus the theoretical amount applied.

Results and Discussion

The size distribution of the core (uncoated) beads is shown in Fig. 4. The data indicate that there are three main fractions and smaller percentages of other sized beads. The bulk density of beads was determined to be 0.8 g/ml.

Sub-batches of these beads were coated using

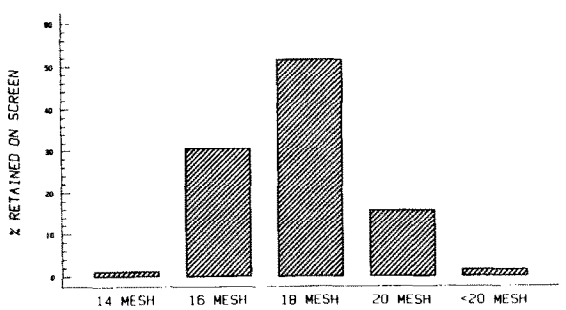

Fig. 4. Size distribution of beads manufactured by extrusion/spheronization (before coating).

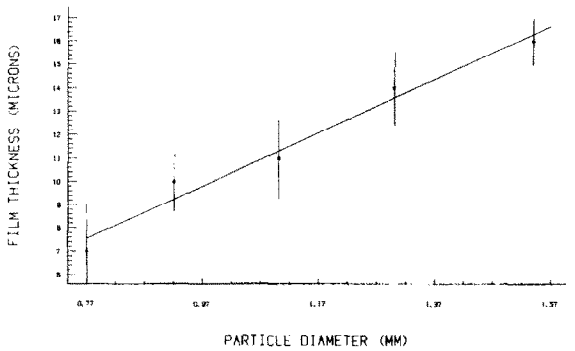

Fig. 5. Average film thickness values ($n = 10$) plotted against median particle diameter of beads of each size fraction coated as a composite batch using the bottom spray mode. Error bars represent a standard deviation of film thickness measurements (SE).

the three spray modes discussed earlier, and film thickness of the various size beads was measured using the SEM. The data are graphically presented in Figs 5–7. The data obtained from the batches coated using the bottom spray mode are consistent with previous reports (Wesdyk et al., 1990); this process produced product which displayed film thickness variation that could be correlated with bead size. The film thickness ranged from a low of about 7 μm on the smallest beads contained within the batch to a high of about 17 μm for the largest beads contained within the same batch. However, as can be noted in Figs 6 and 7, the top and tangential spray mode produced beads that have practically no trend in film

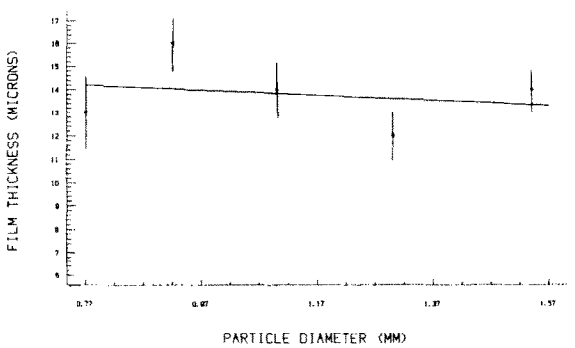

Fig. 6. Average film thickness values ($n = 10$) plotted against median particle diameter of beads of each size fraction coated as a composite batch using the top spray mode. Error bars represent a standard deviation of film thickness measurements (SE).

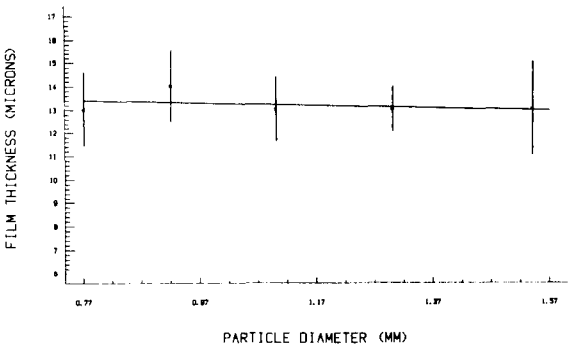

Fig. 7. Average film thickness values ($n = 10$) plotted against median particle diameter of beads of each size fraction coated as a composite batch using the tangential spray mode. Error bars represent a standard deviation of film thickness measurements (SE).

thickness as a function of bead size. The slight variation in the film thickness values obtained from the top spray coated beads is believed to be a result of solubilization of core components into the film. This phenomenon made it difficult to determine the boundary between the core bead and the film, and consequently contributed to the greater variation in the measurement of film thickness. Despite this, in a practical sense it is clear that the film thickness did not vary as a function of pellet size as it had in the case of beads coated in the bottom spray mode.

The trends noted with respect to film thickness variation can be further supported by examining the dissolution characteristics of the coated beads. The various size beads contained in each batch (top, bottom, and tangential spray mode) were screened into separate fractions and encapsulated in no. 1 gelatin shells to yield 100 mg potency capsules. Capsules were also prepared from the composite batch (before screening; containing all size beads). The capsules were subjected to dissolution testing and release rates were estimated, for comparative purposes, from the initial portion of the dissolution curves (Fig. 8) using standard linear regression analysis. The release rates determined were then normalized for surface area differences. As noted by Fick's first law,

$$(1/A)\ \mathrm{d}M/\mathrm{d}T = DK\Delta C/L \qquad (1)$$

where A is the surface area of the bead, D denotes the diffusion coefficient, K is the partition coefficient between the membrane and the core, ΔC represents the concentration gradient across the membrane, and L is the film thickness

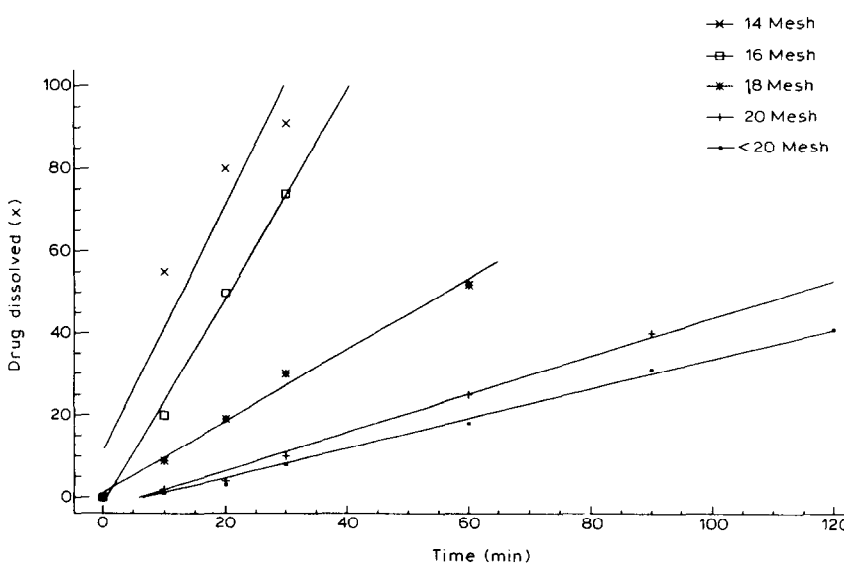

Fig. 8. Regression results of the initial portions of dissolution profiles generated for bottom spray coated beads.

or the diffusion path length. If film thickness was uniform across the size range, then the release rates would be proportional to the surface area of the beads. However, surface area normalized release rates, which are given in Table 2, would be constant, or independent of bead size.

The beads coated in the tangential or top spray modes displayed surface area normalized release rates that are independent of bead size. However, the normalized release rates of the beads coated in bottom spray mode varied with the size of the bead. These results are consistent with the film thickness data previously discussed. The various size beads contained within a single batch, coated using the bottom spray mode, display differences in film thickness that can be correlated with the bead size, while the beads coated in the top or tangential spray modes did not.

Fluidization characteristics, and hence the variability of the film thickness, are governed by the design of the specific spray modes. In the tangential spray mode, fluidizing air, and centrifugal and gravitational forces combine to effect a rope-like helical fluidization pattern of product (Olsen and Mehta, 1985). Hence, the movement of the various size beads is restricted to a fairly narrow band, thereby limiting any potential for segregation. It can be further argued that the well packed fluidized bed present in this system limits differences in particle velocity, and consequently little variation in film thickness should be expected. In the top spray mode, fluidization patterns are much more random than in the tangential or bottom spray mode. In this case, the random nature of the bubbling/spouting bed may limit the potential for segregation or differences in bead velocities.

In the case of the bottom spray mode, differences in the thickness of film deposited on the various size beads have previously been attributed to segregation of the particles as they exited the Wurster column and differences in particle velocities through the coating zone (Wesdyk et. al, 1990). The segregation of the various sized beads occurred as particles exited the Wurster column and decelerated in the expansion chamber. The smaller sized beads were fluidized higher in the expansion chamber. This segregation could cause differences in cycle times to the coating zone, and hence, differences in the amount of film applied over the course of many cycles, or batching. Differences in bead acceleration through the coating zone, or Wurster column, arose as a result of the manner in which the forces acting on the beads were distributed. Modelling of the system indicated that the forces were distributed as a function of a bead's cross-sectional area per unit mass. The larger the cross-sectional area per unit mass, the greater the acceleration through the Wurster column, and consequently less time spent in the spray zone. Therefore, the film thickness would be inversely proportional to the bead's acceleration, or di-

TABLE 2

Average (n = 6) release rates, normalized for surface area of various size beads coated using top [a], bottom, or tangential spray mode

Bead size (mesh)	Total surface area per capsule [b] (cm^2)	Normalized release rate (% drug dissolved/cm^2 per min)		
		Bottom spray	Top spray	Tangential spray
12–14	1.0	0.3	0.8	0.6
14–16	1.3	0.4	0.7	0.5
16–18	1.5	0.7	0.7	0.6
18–20	1.8	1.4	0.9	0.7
20–25	2.1	1.4	0.8	0.7
Composite	N/A	0.7	0.7	0.6

[a] Coating levels adjusted to achieve similar composite dissolution profiles from each spray mode.

[b] Total surface area per capsule was calculated from the median particle radius for each fraction.

rectly proportional to the bead's mass per unit cross-sectional area. The film thickness values were shown to correlate well with this factor.

Examination of the principles affecting the fluidization patterns of the beads indicates that it might be possible, through modification of selected processing parameters, to substantially reduce the level of segregation of the beads while having little impact on the relative differences in acceleration of the particles through the coating zone.

Fluidization is a condition in which the beads are supported by drag forces caused by the air passing through interstices among the particles at some critical velocity. The beads are fluidized to a height at which the velocity of the fluidizing air is less than what is necessary to support the particle. This minimum fluidizing velocity (V_{flmin}) is related to both a particle's size and weight. In the simplest case, in which one ignores wall effects and other complicating factors, the velocity of the fluidizing air can be expressed as a function of the geometry, or more specifically, the diameter, of the coating chamber. This is a simple extension of Bernoulli's Equation, a fundamental relation in fluid mechanics. The geometry of the bottom spray coater utilized for this study (Fig. 1) is such that the diameter of the Wurster column is constant, as is the diameter of the product (lower) chamber. The diameter of the expansion (upper) chamber, however, is increasing, as it is conical in design. If one considers the velocity of the fluidizing air as a function of the column diameter, then the fluidizing air velocity could be represented schematically as in Fig. 9, curve V_1. Assuming the range of minimum fluidizing velocities for the large and small beads given in the plot, it can be seen that segregation would occur as a result of the gradual decrease in the velocity of the fluidizing air in the expansion chamber. If, however, the velocity of the fluidizing air was lowered (from curve V_1 to curve V_2, Fig. 9), through a reduction of the atomizing air pressure or fluidizing air volume, then the range of minimum fluidizing air velocities of the various size beads would fall within the step region, or the area of rapid decrease in fluidizing air velocity, encountered as the product exits the Wurster

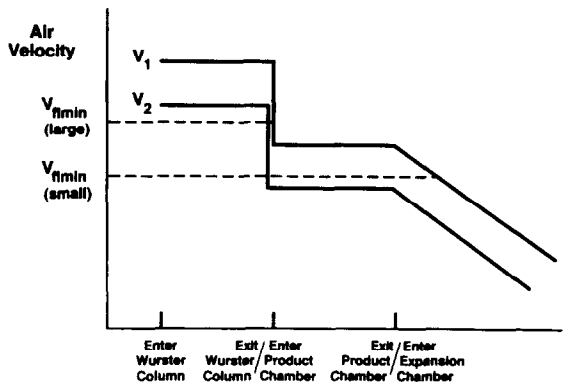

Fig. 9. Fluidizing air velocity expressed as a function of physical regions of a bottom spray coater. Not drawn to scale.

column. Thus, a reduction in the velocity of the fluidizing or atomizing air has the potential to reduce the extent of segregation in a polydispersed bead system.

Theoretically, the reduction in air velocity would not have a substantial impact on the magnitude of the differences in bead acceleration through the coating zone. Previous work (Wesdyk et al., 1990) indicated that a particle's acceleration through the Wurster column (a_{upward}) was related to the affect of gravity and the fluidizing/atomizing air;

$$a_{\text{upward}} = a_{\text{fluidizing air}} - a_{\text{gravity}} \tag{2}$$

The major contributing factor, the acceleration due to the fluidizing/atomizing air, was given as a function of the size and mass of a particle, and the magnitude of the force of the air;

$$a_{\text{fluidizing air}} = F \cdot A/M \cdot K \tag{3}$$

where, F denotes the magnitude of the force of the fluidizing/atomizing air, A is the cross-sectional area of the particle in the direction of motion, M represents the mass of the particle, and K is a constant describing the drag coefficient of the sphere, the density of the gas (air), and the relative velocity between the particle and the air. Eqn 3 indicates that, regardless of the extent of the reduction of the atomizing air pressure or fluidizing air volume, these forces would

still be distributed as a function of a particle's cross-sectional area per unit mass.

In summary, while application of the model shown in Fig. 9 suggests that an appropriate reduction in fluidizing air volume will eliminate segregation of beads as they emerge from the top of the Wurster column, such a reduction in air volume would not influence the differences in acceleration of particles since such differences continue to be influenced by the size and mass of individual particles as predicted by Eqn 3.

A full 2^2 factorial study was used to evaluate the impact of reductions in the atomizing air pressure and fluidizing air volume. Beads were coated, in the bottom spray mode, using 'high' and 'low' settings for the referenced processing parameters, and the film thickness of the various sized beads was measured. Standard linear regression analysis of film thickness values was performed. The slope of the regression line indicates the extent of variation in the film thickness across the size range. The smaller the slope, the less is the variation. The results are given in Table 3. The data indicate that a reduction, by one half, of fluidizing air volume did not have an effect on the variation in film thickness at either atomizing air pressure setting. Utilizing the color coded beads described earlier to monitor fluidization patterns, it was clear that modification of the fluidization air volume also had no substantial effect on the segregation of the various size beads.

The reduction in atomizing air pressure produced only a slight decrease in film thickness variation; as indicated in Table 3, the range in film thickness across the various size beads was not substantially reduced. However, when examining fluidization patterns it was noted that the reduction in atomizing air pressure, regardless of the setting of the fluidizing air volume, did significantly reduce the extent of segregation of the various size beads. At high atomizing air pressures, extremely wide, distinct bands of the various sized beads were visible. At lower atomizing air pressures, no segregation was visible. Thus, it appears that while segregation of the beads, leading to differences in cycle times, does affect film thickness variation, this phenomenon does not play a major role. It should, however, also be noted, that the modification of processing parameters such as atomizing air pressure and fluidizing air volume, while slightly reducing the extent of the variation of film thickness in certain cases, can also impact on the quality film formed with respect to surface morphology (monitored by SEM), extent of solubilization of core components (monitored by EDX), and performance (monitored by dissolution). Similar findings have been previously reported (Brown, 1986; Hossain and Ayres, 1990).

Lastly, it should be noted that there are other advantages and disadvantages associated with each of the three spray modes besides film thickness variation. Specifically, the quality of film formed using top spray mode, and attrition of product due to high shear forces encountered in the tangential spray mode, are of concern. These observations are well documented in the literature (Mehta and Jones, 1985; Olsen and Mehta, 1985).

TABLE 3

Film thickness variation as a function of process parameter setting

Atomizing air setting (bar)	Fluidizing air (CFM)	Slope ± SE (μm/mm)	Correlation coefficient	Film thickness range (μm)	Segregation
1.5	36	9.4 ± 3.4	0.85	15–8	limited
1.5	72	9.6 ± 2.0	0.94	14–7	limited
3.5	36	11.5 ± 0.8	0.99	15–6	extensive
3.5	72	11.7 ± 1.9	0.96	16–7	extensive

Conclusions

Theoretically, the various size beads contained within a batch should display films of similar thickness when coated under ideal conditions. In the present study, however, it was observed that only beads coated in the top or tangential spray mode displayed films of uniform thickness with respect to bead size. Beads coated in the bottom spray mode did not; larger beads displayed thicker films compared to the smaller beads. This variation in film thickness was further supported by examining surface area normalized release rates of the beads.

Previous work (Wesdyk et al., 1990) had related the variation of film thickness observed for beads coated in the bottom spray mode to differences imparted to the fluidization patterns of the product by the design of the spray mode. Two specific potential contributors to the variation in film thickness were noted; segregation of particles leading to differences in cycle times to the coating zone, and differences in particle velocity through the coating zone. Through study of the impact of the modification of selected processing parameters, it was observed that a reduction of the atomizing air pressure in the bottom spray mode, while substantially reducing segregation and differences in cycle times, only had a marginal effect on the variation of film thickness.

This study has demonstrated that the various size beads dispersed in a single batch do receive films of similar thickness when coated under ideal conditions. When film thickness is shown to vary with respect to the size of the beads, as it does when the beads are coated in the bottom spray mode, the film thickness variation can be related to differences imparted to fluidization patterns by the design of the spray mode. Of the two possible contributors noted, the segregation of particles, leading to differences in cycle times, was shown not to be the major factor affecting the film thickness variation. Further work is needed to confirm the impact of proposed variations in particle velocity through the coating zone. It is not clear if the extent of differences in particle velocity, required to cause the observed film thickness variation, could actually occur. While theoretically this is possible, the degree to which the particle bed is packed could limit this phenomenon. The effects of other possible contributors, such as horizontal segregation of beads within the coating zone, also needs to be investigated.

The presence of film thickness variation and its effect on the dissolution characteristics of the beads coated in the bottom spray mode, combined with the potential for segregation, during encapsulation, of the various size particles of a free flowing beadlet system, point to the need to limit the extent of particle size variation of the starting product through optimization of the bead making process.

References

Brown, D.T., Semiquantitative investigation of tablet coats by electron probe microanalysis. *Drug Dev. Ind. Pharm.*, 12 (10) (1986) 1395–1418.

Ghebre-Sellassie, I., Gordon, R.H., Middleton, D.L., Nesbitt, R.U. and Fawzi, M.B., A unique application and characterization of Eudragit E 30 D film coatings in sustained release formulations. *Int. J. Pharm.*, 31 (1986) 43–54.

Hossain, M. and Ayres, J., Variables that influence coat integrity in a laboratory spray coater. *Pharm. Technol.*, 10 (1990) 72–82.

Mehta, A.M. and Jones, D.M., Coated pellets under the microscope. *Pharm Technol.*, 9 (1985) 52–60.

Olsen, K.M. and Mehta, A.M., Fluid bed agglomeration and coating technology – state of the art. *Int. J. Pharm., Tech. Prod. Mfg*, 6 (4) (1985) 18–24.

Ragnarsson, G. and Johnsson, M.O., Coated drug cores in multiple unit preparations; influence of particle size. *Drug Dev. Ind. Pharm.*, 14 (1988) 2285–2297.

Wesdyk, R., Joshi, Y.M., Jain, N.B., Morris, K., and Newman, A., The effect of size and mass on the film thickness of beads coated in fluidized bed equipment. *Int. J. Pharm.*, 65 (1990) 69–76.